Spatial-Temporal Queuing Theoretic Modeling of Opportunistic Multi-hop Wireless Networks With and Without Cooperation

Dibakar Das, *Student Member, IEEE,* and Alhussein A. Abouzeid, *Senior Member, IEEE*

Abstract

In this paper, we characterize the average end-to-end delay in an opportunistic multi-hop secondary cognitive radio network overlaid with a primary multi-hop network. Nodes in both networks use random medium access control (MAC) scheme with exponentially distributed back-off. We first model the network as a two-class priority queuing network and use queuing-theoretic approximation techniques to obtain a set of relations involving the mean and second moments of the inter-arrival time and service time of packets at a secondary node. Then, applying these parameters to an equivalent open single-class G/G/1-queuing network, we obtain expressions for the average end-to-end delay of a packet in the secondary network using a diffusion approximation. Next we extend the analysis to a case where secondary nodes cooperatively relay primary packets so as to improve their own transmission opportunities. The mathematical results are validated against extensive simulations.

Index Terms

Cognitive radio, cooperation, relay, queueing theory, queuing delay, 802.11.

I. Introduction

The exponential growth in the number and demand of wireless devices has motivated the study of new techniques to be implemented in future wireless networks. Such techniques include new spectrum sharing regulatory rules allowing real-time sharing of licensed but unused spectrum, and new proposals for dynamic spectrum sharing that leverage the recent advances in software/ cognitive radio technologies, promising to provide better spectrum utilization and agility [1], [2].

In this work we consider the coexistence of two multi-hop wireless networks, one composed of licensed primary users (PUs) and the other composed of lower priority opportunistic secondary users (SUs) that possess spectrum-agile functionalities. We investigate the average end-to-end delay in the secondary network. Both networks use a random access MAC protocol similar to collision avoidance mechanism of IEEE 802.11 random access protocols. The average end-to-end delay is the end-to-end delay averaged over all received packets and network topologies and it depends on the traffic pattern, number of nodes, MAC scheme and routing protocol. To the best of our knowledge, no previous work (except our preliminary work in [3]) addressed the average end-to-end delay in such a setting. We introduce a modified protocol model of interference to account for packet loss during transmission due to fading. We consider two cases. In the non-cooperative case, there is no cooperation between the two networks. In the cooperative case, we consider a protocol wherein secondary nodes relay primary packets that were not correctly received at a primary receiver but were successfully received at a nearby secondary node. Such end-to-end delay analysis is relevant especially in the context of future multihop cellular networks that consists of several small cells. In such cases, due to small coverage area of the base-stations associated with such cells, multi-hop operation is expected to be commonly adopted [4]–[6].

D. Das is with the Department of Electrical and Computer Engineering, Rensselaer Polytechnic Institute, Troy NY 12180 USA (e-mail: dasd2@ rpi.edu). A. A. Abouzeid is with the Department of Electrical and Computer Engineering, Rensselaer Polytechnic Institute, Troy NY 12180 USA, and a visiting Professor with the Centre for Wireless Communications, University of Oulu, Oulu 90014, Finland (e-mail: abouzeid@ecse.rpi).

Manuscript received July 22, 2014; revised April 26, 2015.

In this paper we investigate how the end-to-end delay depends on number of nodes and traffic patterns under both cooperative and non-cooperative protocols. The main result of this paper is the application of queuing theoretic techniques for deriving approximate mathematical expressions for:

1) The average end-to-end delay of secondary packets for the non-cooperative as well as the cooperative case.
2) The maximum achievable throughput of primary and secondary users under both cooperative and non-cooperative protocols, and conditions under which each type of user benefits from cooperation (in terms of throughput).

The solutions for the average end-to-end delay for both cooperative and non-cooperative protocols have closed form expressions except for terms corresponding to the average probability of successful transmission from primary and secondary users. Those terms are obtained using numerical integration. From simulation results we observe that the approximation matches closely with experimental results for low to moderate channel utilization, where channel utilization is precisely defined later in the paper.

The methodology in this paper can be summarized as follows. For both cooperative and non-cooperative scenarios we first model the network as an open network of two-class G/G/1 pre-emptive resume service First Come First Serve (FCFS) priority queues. We then use certain queuing approximation techniques from [7] to find relations involving the effective service time and inter-arrival time of packets at every node. Transmissions from interfering neighbors (to be defined later) constitute high-priority class-1 traffic at every station. Self-generated or forwarded packets from other nodes and unsuccessful packet transmission attempts by a node constitute arrival of lower priority class-2 traffic at the corresponding station. Next we model the network as a collection of single-class G/G/1 (non-priority) queues for which the effective service time and the inter-arrival time of a job at any station satisfies the corresponding relations for class-2 jobs in the priority queuing network representation (obtained in the first step). This enables the derivation of expressions for the average end-to-end delay using diffusion approximation for an open queuing network consisting of G/G/1 stations as given in [8].

There exists several related works on queuing delay in cognitive networks. In [9], the authors analyze queuing delay *in a single-hop* network of multiple SUs that uses random access, in presence of multiple primary channels by using continuous fluid-queue approximation. In [10], the authors study delay performance of one SU in the presence of other PUs sharing the same channel. They propose a time-threshold scheme for SU packet transmission by developing a Markovian model wherein each state is the number of SU packets at the beginning of every idle time-slot. In [11] the authors model the primary user activity as an ON-OFF alternating renewal process and used M/G/1 queuing analysis to obtain the average delay for a single secondary user in presence of primary activity. In [12] the authors use a priority queue model to analyze delay performance of a secondary user with multiple classes of traffic. In [13] the authors use M/D/1 priority queueing scheme to obtain the average delay for primary and secondary users. In [14], the authors use pre-emptive priority queuing system to evaluate the average waiting time of delay-sensitive and delay-insensitive packets for two cases- (a) multiple PUs and a single SU where the SU senses only at the beginning of a time-slot and (b) a single PU and a single SU where the SU senses the channel continuously. Other works such as [15], [16] also analyze delay for single-hop SUs by using a priority queue model for channel access. However, none of these works [9]–[16] study delay in a multi-hop network. While we use a similar priority queue-model as [13]–[16], in our case the service time process of an SU is interrupted due to transmission process of nearby PUs and SUs and the latter in turn depends on their own respective service time processes. As a result, our scenario is different from that in previous works. In [17], the authors characterize the minimum multi-hop delay and connectivity of the secondary network as a function of SU and PU densities. However, this work also does not address the scenario where different secondary nodes are contending for the channel.

Our cooperation model is similar to other works such as [18]–[26] where secondary users cooperatively relay primary packets. In [18] the authors consider two links: a primary and a secondary; a secondary relay node re-transmits packets that were correctly received at the relay node but not successfully received by the intended primary destination node. A similar model is used in [19] wherein the authors consider a single

primary source-destination (s-d) pair in the presence of multiple secondary nodes that can act as relay. In addition, the queued primary packets at the relay nodes are transmitted with a higher priority in every idle slot. In [20] the authors consider a primary s-d pair aided by a cognitive cluster of one or more nodes. The authors consider 4 different cooperation schemes; under 2 of those protocols a secondary node can use dirty-paper coding technique to simultaneously transmit secodary packets when another secondary node relays a primary packet. In [21] the authors obtain stable throughput region for the primary and secondary users in a network consisting of 5 nodes with 2 primary transmitters and one common secondary relay. In [22] the authors consider uplink of a Time Division Multiple Access (TDMA)-based primary network where some cognitive nodes assist the primary network by re-transmitting some primary packets that were not received successfully at the base-station. In [23] and [24] the authors consider cooperation between a primary user and a relaying secondary user such that the secondary rate is maximized subject to stability of the primary queue. Under the proposed protocol in [23] the primary queueing delay with cooperation is less than that without cooperation and average energy emitted by the secondary user is below a certain threshold. Under the proposed protocol in [24] the primary user cooperates with secondary user if and only if the average number of transmitted primary packets per unit energy is higher with cooperation than without. In [25] the authors find optimal cooperative power allocations in a network of multiple secondary users and a single primary user. However the authors only consider primary packet generation rates for which the network is stable even without cooperation. In [26] the authors extend the work in [25] to include cases of higher primary packet arrival rates. However none of the above works looked at the average delay of secondary packets in a multi-hop scenario.

Our network model is based on that in [27] where the authors obtain closed form expression for the average end-to-end delay in a multi-hop network of nodes that use a random-access MAC and probabilistic routing protocol. The authors first obtained exact expressions for the mean and second moments of the effective service time of packets exploiting the simplistic nature of the routing protocol and MAC scheme. Then they used a diffusion approximation for single-class G/G/1 systems to obtain closed form expressions for the average end-to-end delay. *In contrast* to [27] which considered a single network, this work considers two co-existing and interacting networks (primary and secondary) where nodes from one network (i.e. primary) have higher priority of channel access than the nodes from the second network (i.e. secondary). This coupling of the behavior of the queues in the two networks introduced new modeling challenges, which are analyzed by applying new approximation techniques that have not been used before in this context.

In the next section, we describe the multi-hop cognitive radio network model. Section III briefly discusses the theoretical queuing network results on diffusion approximation for priority queues [7] and the diffusion approximation for non-priority single-class G/G/1 systems [8], which are used in later sections. In Section IV we derive expressions for the average end-to-end delay for secondary packets without cooperation. In Section V we derive expressions for the average end-to-end delay for secondary packets with cooperation. In Section VI we discuss when cooperation benefits primary and secondary users. In Section VII, we compare the analytical and simulation results and find that they closely match for wide range of channel utilization scenarios. Section VIII concludes the paper. Due to lack of space we only provide the relatively significant proofs (that of Theorem 1 and Lemma 4); proofs of other lemmas, Theorem 2 and Corollary 1 can be found in our technical report [28].

II. Network model

In this section we present the model of multi-hop primary and secondary ad-hoc network first for the case where the primary and secondary nodes do not cooperate with each other and then for the case where the secondary nodes cooperatively relay primary packets. Both networks share a single channel. We assume the primary and secondary networks consist of $n^{(p)}+1$ and $n^{(s)}+1$ nodes respectively. Nodes are distributed uniformly and independently over the surface of a torus of unit area. The surface of the torus can be viewed as a planar disk of unit area wrapped around itself. We select the torus to simplify the analysis without considering edge-effects.

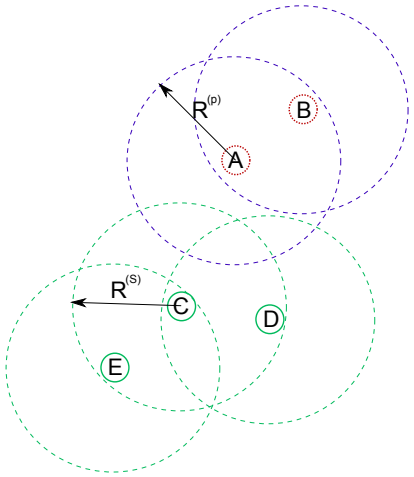

Fig. 1. A network with two primary nodes: A,B and 3 secondary nodes: C,D and E. A and B are both transmission and interfering neighbors to each other. C, D and C, E are transmission neighbors to each other. Interfering neighbors of C are D,E and A. Interfering neighbors of D are C,E and A. Interfering neighbors of E are D and C.

A. Network Model for Non-cooperative Case

In the following subsubsections we discuss the channel model, interference model, routing model and the MAC behavior for the case where secondary nodes do not cooperate with primary nodes. We also present a queuing network representation of the network.

1) Channel Model

The wireless channel between a transmitting node and its destination is subjected to Rayleigh fading with additive white noise at the receiver. We assume block fading where the fading coefficients are independent among different transmission links and different transmission attempts. Let d_{ij} and h_{ij}^t denote the distance between node i and j and the channel fading coefficient between i and j at time t, respectively. h_{ij}^t is a zero mean independent and identically distributed (i.i.d.) complex Gaussian random process with variance σ_0^2; it remains constant during every packet transmission time. The signal received at a receiver j from a node i at time t, denoted as Y_{ij}^t, can be modeled as [22]:

$$Y_{ij}^t = \sqrt{\psi_i d_{ij}^{-\vartheta}} h_{ij}^t S_i^t + F_{ij}^t \tag{1}$$

where ψ_i denotes the transmission power of i, ϑ denotes the path-loss exponent, S_i^t denotes the signal of unit power transmitted by i at time t and F_{ij}^t denotes an i.i.d. zero mean white Gaussian noise at j with variance N_0. A packet transmission is successful if the instantaneous signal-to-noise-ratio (SNR) at the receiver is above a specified threshold θ. The probability of this event is therefore [22],

$$P(\text{SNR at } j \geq \theta) = \exp(-\frac{N_0\theta}{\psi_i \sigma_0^2 d_{ij}^{-\vartheta}}). \tag{2}$$

2) Interference Model

In order to account for packet-loss due to fading and simultaneously ensure tractable analysis we use a modified version of the Protocol Model of interference described in [29]. In the protocol model, a successful transmission occurs if and only if the receiver is within the transmission range of the transmitter and outside the interference range of other nodes that are transmitting simultaneously. Thus, the effect of interference is determined based only on whether the receiver is within interference range of simultaneously transmitting nodes other than the transmitter in question. Using a modified protocol model of interference we capture the effect of channel fading between a transmitter-receiver pair on the received SNR while ignoring interference from adjacent nodes. This leads to tractable analysis. Details about the model is presented next.

Every primary (respectively secondary) node transmits at equal power. With slight abuse of notation we reuse the symbol ψ to denote the transmission power of every primary and secondary node as $\psi^{(p)}$

and $\psi^{(s)}$ respectively. A primary (or secondary) node can only transmit to other primary (or secondary) nodes within its transmission radius $R^{(p)}$ (or $R^{(s)}$) and the transmission is successful if the received SNR is higher than θ. All primary (or secondary) nodes located within transmission radius of a given primary (or secondary) node are called *transmission neighbors* to that node. We assume $R^{(p)}$ and $R^{(s)}$ are such that both primary and secondary networks are connected.

A primary (or secondary) node i can transmit to its transmission neighbor j only if no other node k, such that j is within transmission radius of k, is transmitting simultaneously. Accordingly we define *interfering neighbors* of k as the set of all nodes whose transmissions may collide with that of k. Primary (or secondary) interfering neighbors to a primary (or secondary) node k are all primary (or secondary) nodes located within distance $2R^{(p)}$ (or $2R^{(s)}$) from k. Note, a primary (or secondary) interfering neighbor can be located at most $R^{(p)}$ (or $R^{(s)}$) distance away from the intended primary (or secondary) receiver. If k is a secondary node, primary interfering neighbors of k are all primary nodes located within distance $R^{(p)} + R^{(s)}$ from k. A node freezes its backoff timers and pauses any ongoing transmission activity if any of its interfering neighbors starts transmitting. Note that primary nodes do not have any secondary interfering neighbor since they have higher priority of channel access than secondary nodes.

Definition of interfering neighbors is same as that in [29] obtained by setting a guard-zone parameter Δ in [29] to zero[1]. For convenience of analysis we set Δ as zero. The analysis in this paper can be easily extended to case of non-zero Δ.

The above transmitter-centric model simplifies the analysis even though it provides a more conservative estimate of feasible concurrent transmissions than a receiver-centric approach. Also, this model alleviates the need to study the hidden terminal problem. In IEEE 802.11 protocols the Request to send (RTS)/Clear to send (CTS) mechanism is used to solve the hidden terminal problem.

3) Packet Generation and MAC Model

Every primary and secondary node generates packets at a rate $\lambda^{(p)}$ and $\lambda^{(s)}$ packets/second, respectively. The size of a packet is constant and is equal to L bits.

The backoff mechanism is based on IEEE 802.11 collision-avoidance mechanism and does not factor in the effect of collisions. Nodes in both networks use random access MAC with exponential back-off timers[2]. The mean durations of the back-off timer is denoted as $\frac{1}{\xi}$[3]. If a packet transmission from any node is unsuccessful, the packet remains at the head of its transmission queue. The transmission queue is a link-layer queue.

We assume an ideal sensing process, i.e. the secondary nodes can sense transmission activity of primary interfering neighbors almost instantaneously[4] and pause any of their ongoing transmission processes. We assume a given primary node listening for the channel activity can differentiate between channel usage by primary and secondary nodes. If a primary node, which has high priority of channel access, senses that the channel is being used by a secondary node, it still treats the channel as if it is idle i.e. its backoff process is not affected. The secondary nodes will sense the channel once transmission from primary node is over and before resuming transmission of remaining bits.

The transmission rate of both primary and secondary nodes is W bits/second. The transmission time of every packet is $\frac{L}{W}$ seconds, ignoring the time required to exchange RTS, CTS and acknowledgement (ACK) packets.

[1]According to [29], in a homogeneous network a node X_i transmits successfully to another node X_j on the same channel if $|X_k - X_j| \geq (1+\Delta)|X_i - X_j|$ for every node X_k simultaneously transmitting on the same channel. Here, $|X_k - X_j|$ and $|X_i - X_j|$ denote the distance between X_j and X_k and between X_i and X_j respectively. The parameter $\Delta > 0$ accounts for imprecision in transmission range.

[2]The assumption of exponential distributions is motivated by [30]. In [30] authors exploit the memoryless property of exponential distributions to show that this assumption leads to tractable analysis for IEEE 802.11 networks. Results obtained using their model were found to be highly accurate in predicting behavior of the IEEE 802.11 MAC protocol.

[3]In general ξ is not constant but depends on number of contending nodes. However, in this work we assumed there is no collision under the ideal sensing mechanism and hence ξ is constant and is equal for all nodes.

[4]In practice, if virtual carrier sensing is employed, sensing time is determined by transmission time of RTS and CTS packets. However, transmission time of such packets are low compared to that of data packets (due to smaller size) which is why we assumed ideal sensing.

4) Routing Model

We assume a probabilistic routing model for both primary and secondary nodes. On receiving a packet from one of its transmission neighbors, a primary (or secondary) node absorbs it with probability $q^{(p)}$ (or $q^{(s)}$) or forwards it to a transmission neighbor, picked with equal probability among all transmission neighbors, with probability $1-q^{(p)}$ (or $1-q^{(s)}$). This selection is independent of past history of packet transmission attempts i.e. whether or not a previous transmission to a given node was successful. The variables $q^{(p)}$ and $q^{(s)}$ model locality of traffic between the source and destination of transmitted packets and are functions of node densities. Higher $q^{(p)}$ (or $q^{(s)}$) means, on average, source-destination pairs in the primary (or secondary) network are connected via lower number of hops and vice versa.

5) Queuing Network Representation

We represent the network as an open 2-class queuing network of G/G/1 FCFS pre-emptive resume service priority queues. Each station of the network corresponds to a node. Throughout the paper we use the terms "node" and "station" interchangeably whenever there is no confusion. This queuing network model accounts for interruptions in the on-going service of a packet (includes the durations of both the back-off timer and the transmission time) due to transmission from interfering neighbors. All such transmission activities are modeled as high priority class-1 jobs. Since, the duration of every interruption event is the packet transmission time $\frac{L}{W}$, the service time of any class-1 job is $\frac{L}{W}$[5]. Low priority class-2 jobs correspond to physical packets present at any node. Their service time is equal to the sum of transmission time and duration of backoff timer; therefore, without interruption each class-2 job would have been served at rate $\frac{1}{\frac{L}{W}+\frac{1}{\xi}}$. The model can be summarized as follows:

1) The transmission process from all interfering neighbors constitute a *virtual* arrival process of higher priority class-1 jobs at any station. This process is approximated as the *sum* of the transmission process from those nodes[6]. Those processed virtual jobs are then forwarded to a sink with probability 1.
2) Following events constitute arrival process of class-2 jobs at any station i: a packet is generated at i (modeled as external arrival process of class-2 jobs at station i), a transmission neighbor forwards a packet to i and it is not absorbed, and a packet transmission attempt from i is unsuccessful. Every station forwards processed class-2 jobs as both class-1 and class-2 jobs to other stations. We denote as $r_{ij}^{(k,l)}$ the probability that a class-k job at station i is forwarded as a class-l job to station j. All processed class-2 jobs from station i are forwarded with probability 1 to every station j for which i is an interfering neighbor i.e. $r_{ij}^{(2,1)}=1$. Recall, every packet is transmitted to one of the transmission neighbors picked randomly and the transmission is successful only if the SNR at the receiver is greater than or equal to θ. Hence, every class-2 job from i is forwarded with probability $r_{ik}^{(2,2)}$ to a transmission neighbor k where

$$\begin{aligned} r_{ik}^{(2,2)} &= \frac{P(\text{SNR at } k \geq \theta)}{\text{Number of neighbors of } i} \\ &\times \; P(\text{packet is not absorbed at } k). \end{aligned} \tag{3}$$

A processed class-2 job from station i is forwarded back to i with probability $r_{ii}^{(2,2)} = 1-\sum_{k\neq i}\frac{r_{ik}^{(2,2)})}{1-q^{(p)}}$ if i is primary and $r_{ii}^{(2,2)} = 1-\sum_{k\neq i}\frac{r_{ik}^{(2,2)})}{1-q^{(s)}}$ if i is secondary. Since the primary nodes do not forward secondary packets and vice-versa, we have $r_{ij}^{(2,2)}=0$ if either i or j is a primary node and the other one is a secondary node.

The priority queuing network representation of the network in Fig 1 is shown in Fig. 2.

[5]In a practical network, service time will also account for packet retransmissions due to collisions. However, under our ideal sensing assumptions, there is no collision and as a result service time of virtual jobs is simply the packet transmission time. This assumption facilitates tractable analysis. Similar to observations in [27], we expect the network model to match that of a realistic network for lightly loaded scenarios where there are few collisions and provide an optimistic bound for very high packet generation rates.

[6]This is an approximation because in practice multiple interfering neighbors may transmit at the same time. As a result the overall duration of interruption events at any node is lower than sum of transmission times of its interfering neighbors.

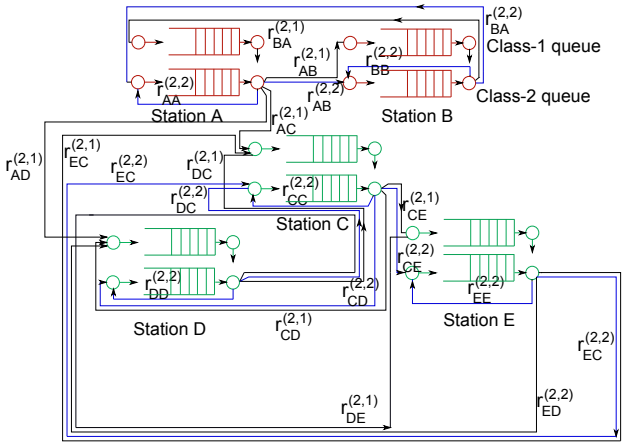

(a) Representation of the network in Fig 1 as a priority queuing network. Each station consists of 2 queues: high priority class-1 queues and low priority class-2 queues. Black and blue lines denote routing of class-1 and class-2 jobs respectively.

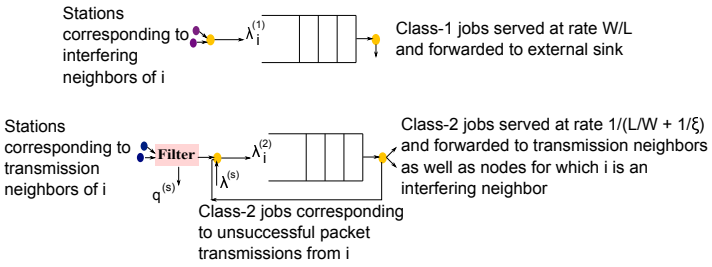

(b) Representation of a node i in the secondary network as a station in the priority queuing network. Served class-1 jobs are routed to an external sink. $\lambda_i^{(m)}$ denotes the arrival rate of a class-m (where m=1,2) job at i.

Fig. 2. Priority-queuing network model representation of the network in Fig 1.

The novelty of the model is in the introduction of virtual or class-1 jobs to capture interruption of service process of any node due to transmission from its interfering neighbors. We emphasize virtual jobs at any station do not represent real packets stored at that node (hence the name "virtual"). The virtual jobs are immediately transferred to an external sink after processing.

Similar to [27], once the overall service time process of class-2 jobs is known, the network can also be modeled as a single class G/G/1 queuing network. Each job in this network correspond only to class-2 jobs in the priority queuing network representation. For the example in Fig 1 the G/G/1 queuing network representation is shown in Fig. 3. In Fig 3a the routing probabilities of jobs are the same as that of class-2 jobs in the priority queueing network representation and for consistency are denoted using same notations.

B. Network Model for Cooperative Case

We now discuss the network model for a cooperative protocol. Consider the event where transmission from a primary node to another fails but a nearby secondary node, close to the primary receiver, successfully receives the packet. Consequently, the probability of successful transmission of a primary packet from the secondary node to the primary receiver is very high. If the secondary node relays the primary packet it may reduce the fraction of time the channel is occupied by primary users thereby creating more transmission opportunity for secondary users.

The channel model, interference model, and packet generation remain the same as in the non-cooperative case (Section II-A). Each primary (or secondary) node transmits a primary (or secondary) packet to one of its transmission neighbors, picked randomly, where it is absorbed with probability $q^{(p)}$ (or $q^{(s)}$). Practically, algorithms exist that utilize random forwarding for routing, such as spray and wait and rumor routing [31], [32]. The detailed cooperative protocol is presented next.

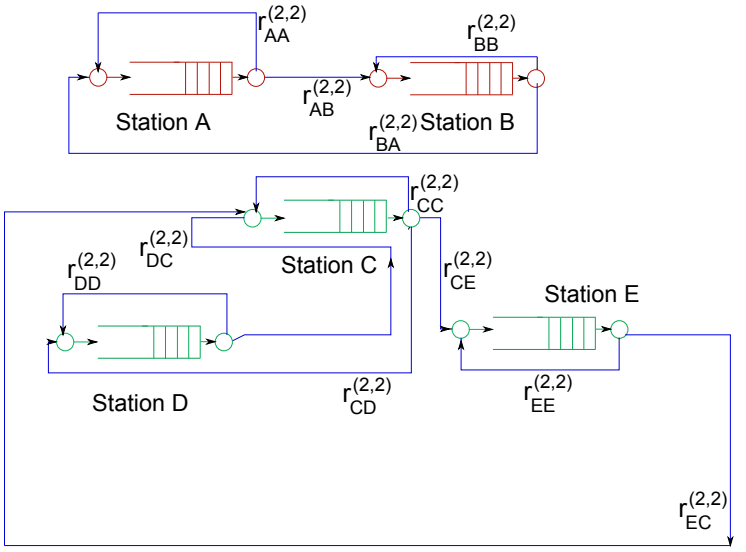

(a) Representation of the network in Fig 1 as a single-class G/G/1 queuing network.

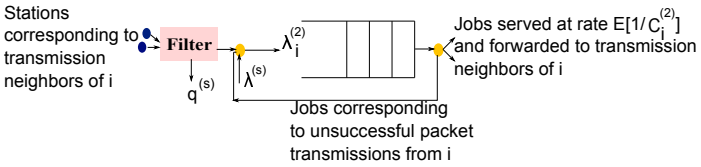

(b) Representation of a node i in the secondary network as a station in the G/G/1 queuing network. Effective service time of a job at station i is same as that of a class-2 job in the priority queuing network representation, denoted as $c_i^{(2)}$.

Fig. 3. Single-class G/G/1 queuing network model representation of the network in Fig 1.

1) Cooperative Protocol

The cooperative protocol model can be described as follows:

1) For any two primary transmission neighbors i and j, only secondary nodes located at distance less than or equal to d_{ij} from i and within a distance d_{rel} (where $d_{\text{rel}} \leq R^{(s)}$) from j are allowed to relay failed primary packet transmissions from i to j. We refer to such secondary nodes as relays of the pair (i, j). The probability of successful transmission from i to any such relay k is at least as high as that from i to j since $d_{ik} \leq d_{ij}$. Moreover, selecting small d_{rel} ensures very high probability of successful transmission from relay node to j (but reduces the number of possible relays).
2) Consider the event: packet transmission from i to j is unsuccessful but one or more relays of (i, j) receives this packet successfully. In this case, exactly one of those relays, randomly picked, sends an ACK packet back to the primary transmitter. The ACK reception is assumed to be collision-free and instantaneous.
3) We assume an ACK is transmitted instantaneously and received correctly by i and other relays. On hearing the ACK all those relays and i drop the packet. The sender of the ACK buffers the packet into its transmission queue. This packet will eventually be relayed to j.
4) Both primary and secondary packets are transmitted in FCFS manner by relay nodes.

Note that secondary relay nodes need to know their distance from nearby primary nodes. Nodes can obtain this information by exchanging information about their locations. Each node can obtain its own location by using a GPS device or range-finding using ultrasonic pulses [33].

2) Queuing Model

The queuing network representation is same as in Section II-A except for the following difference: since some secondary nodes can relay primary packets, $r_{ik}^{(2,2)}$ and $r_{ki}^{(2,2)}$ are no longer zero for every primary

node i and secondary node k.

This cooperation scheme can benefit primary nodes in terms of higher throughput when the secondary network is dense resulting in higher average secondary relay nodes per primary transmitter-receiver pair. In terms of delay, such cooperation may not benefit primary nodes because secondary nodes do not transmit primary packets with higher priority. It is possible to extend our analysis to the case where secondary nodes will transmit primary packets with higher priority over the secondary packets queued at that node. In such case, the priority queuing network model will have three classes of jobs: where class-1 jobs at any station correspond to virtual jobs as before, while class-2 and class-3 jobs correspond to primary and secondary packets stored at that node respectively. For simplicity, we study only the non-priority cooperative scheme.

III. Diffusion approximation for queuing networks

In this section, we give a brief overview of the diffusion approximation techniques used in our work, namely, the diffusion approximation for a general single-class G/G/1-FCFS network (non-priority) [8] and the diffusion approximation for priority queues [7]. The diffusion approximation is a useful technique to derive closed form expressions for the average end-to-end delay in a queuing network. In [8] a diffusion approximation method is used to obtain the average number of packets stored at any station in an open G/G/1 queuing network. Recently in [7] the authors proposed a diffusion approximation solution for multi-class priority queuing networks with preemptive-resume service. We first use approximation techniques in [7] to obtain statistics of the completion time[7] of class-2 jobs and then use the diffusion approximation from [8], to derive the average delay of secondary packets at each node. More detailed review of those diffusion approximation techniques can be found in [28].

A. Diffusion Approximation for G/G/1- queuing Network

Consider a network of n stations with G/G/1 queues numbered from 1 to n. Let Q_i denote the number of jobs at station i (where $1 \leq i \leq n$). We denote the coefficient of variation of inter-arrival times of jobs at i as C_{Ai}. The external arrival process of jobs to the network has mean inter-arrival time $\frac{1}{\lambda}$ and coefficient of variation C_A. The service time at i has mean $\frac{1}{\mu_i}$ and coefficient of variation C_{B_i}. The mean number of jobs at i is given as,

$$\bar{Q}_i = \frac{\rho_i}{1-\hat{\rho}_i} \tag{4}$$

where $\rho_i = \frac{\lambda e_i}{\mu_i}$, $\hat{\rho}_i = \exp(-\frac{2(1-\rho_i)}{C_{Ai}^2 \cdot \rho_i + C_{Bi}^2})$ and $C_{Ai}^2 = 1 + \sum_{j=0}^{n}(C_{Bj}^2 - 1)p_{ji}^2 e_j e_i^{-1}$. The variable e_i denotes the mean number of visits of a job to i and satisfies $e_i = p_{0i} + \sum_{j=1}^{n} p_{ji}(n)e_j$. The variable p_{0i} denotes the probability that a job entering the network from outside first enters i, p_{ji} denotes the probability that a job completed by station j is transferred to i and $C_{B0}^2 = C_A^2$.

B. Diffusion Approximation for Priority Queues

In [7], the authors consider a pre-emptive resume G/G/1-FCFS priority queuing network of M stations, numbered from 1 to M, with K classes of jobs indexed as $1, 2, \ldots, K$. A job of the l-th class (where $1 \leq l < K$) has higher priority than a job belonging to $(l+1)$-th class.

Let $a^{(k)}$, $b^{(k)}$, $c^{(k)}$ and $f^{(k)}$ denote the inter-arrival time, service time, completion time and inter-departure time respectively of a k-th class job (where $1 \leq k \leq K$) in a station in a multi-class network. The change in total number of jobs of class $1, 2, \ldots, K$ at any station during the time-period $[0, t]$ is approximated to be normally distributed with mean $\beta^{(K)}t$ and variance $\alpha^{(K)}t$ where $\beta^{(K)}$ and $\alpha^{(K)}$ are known functions of $\lambda^{(k)}$, $C_A^{(k)}$, $\mu^{(k)}$ and $C_B^{(k)}$. Here $\lambda^{(k)}$, $C_A^{(k)}$, $\mu^{(k)}$ and $C_B^{(k)}$ denote the arrival rate, co-efficient of variation of inter-arrival time, service-rate and co-efficient of variation of service time of a k-th class job in a station in the network respectively.

The probability density function (pdf) of completion time $c^{(k)}$ is approximated, for every $k \in \{1, \ldots, K\}$, as,

$$\varrho_{c^{(k)}}(t) = \int_0^\infty \varrho_{b^{(k)}}(t)\nu^{(k)}(t-T|T)1(t-T)\mathrm{d}T \tag{5}$$

[7]Completion time of a job is defined as the time-period between the beginning and end of service of a job. Clearly, it is same as service time for the highest priority-class, but is greater than service time for other classes.

where

$$1(t) = \begin{cases} 0, \text{ if } t < 0 \\ 1 \text{ otherwise.} \end{cases} \tag{6}$$

Here, ϱ_X denotes the pdf of a random variable X and $\nu^{(k)}$ denotes the pdf of sum of duration of all breaks within the service time T of a class k job at a station due to arrival of a high priority job. The authors approximate $\nu^{(k)}$ in terms of the pdf of duration of each such break, denoted as $\gamma^{(k-1)}$, and the mean, second moment of jobs of class higher than k. The authors also approximate the mean and second moment of each such break in terms of $\alpha^{(k-1)}$ and $\beta^{(k-1)}$.

The pdf of the inter-departure time of class-k jobs (where $1 \leq k \leq K$) is approximated as,

$$\begin{aligned} \varrho_{f^{(k)}}(t) &= \frac{\rho^{(k)}}{1-\tilde{\rho}^{(k-1)}} \varrho_{c^{(k)}}(t) \\ &+ (1 - \frac{\rho^{(k)}}{1-\tilde{\rho}^{(k-1)}})[(1-\tilde{\rho}^{(k-1)}) \varrho_{a^{(k)}}(t) * \varrho_{c^{(k)}}(t) \\ &+ \tilde{\rho}^{(k-1)} \varrho_{a^{(k)}}(t) * \gamma^{(k-1)}(t) * \varrho_{c^{(k)}}(t)] \end{aligned} \tag{7}$$

where $\tilde{\rho}^{(k)} = \sum_{l=1}^{k} \rho^{(l)}$, $\rho^{(l)} = \frac{\lambda^{(l)}}{\mu^{(l)}}$ for every $l \in \{1, \ldots, K\}$ and '*' denotes the convolution operation. The squared coefficient of variation of inter-arrival time of a l-th (where $(l \in \{1, \ldots, k\})$ class job at j, ${C_{Aj}^{(l)}}^2$, is expressed as a function of inter-departure times of jobs routed to station j as,

$$\begin{aligned} {C_{Aj}^{(l)}}^2 &= \frac{\sum_{i=1}^{M} \sum_{k=1}^{K} r_{ij}^{(k,l)} \lambda_i^{(k)} [({C_{Di}^{(k)}}^2 - 1) r_{ij}^{(k,l)} + 1]}{\lambda_j^{(l)}} \\ &+ \frac{{C_{0j}^{(l)}}^2 \lambda_{0j}^{(l)}}{\lambda_j^{(l)}}, \end{aligned} \tag{8}$$

where $\lambda_j^{(l)}$ denotes the arrival rate of l-th class jobs at j, ${C_{Di}^{(k)}}^2$ denotes the squared coefficient of variation of inter-departure time of a k-th class job from station i; $\lambda_{0j}^{(l)}$ and ${C_{0j}^{(l)}}^2$ denotes the average arrival rate and squared coefficient of variation of inter-arrival time respectively of a job of class l at j from a station external to the network.

IV. Delay analysis for non-cooperative protocol

In this section, we find the average end-to-end delay when there is no cooperation between primary and secondary nodes. In Lemmas 1, 2 and 3 we find the average routing probability, arrival-rate of class-2 jobs at any station in the priority queuing network representation and the average number of primary and secondary interfering neighbors to any node respectively. Then in Theorem 1 we use these values along with approximation results from [7] and [8] to derive the average end-to-end delay.

Recall $r_{ij}^{(2,2)}$ denotes the routing probability of a class-2 job from station i to j.

Lemma 1: If i and j are two primary nodes, the expected probability that a class-2 job is forwarded from station i to j is given as,

$$\bar{r}_{ij}^{(2,2)} = \begin{cases} \frac{(1-q^{(p)})\{1-(1-A_{R^{(p)}})^{n^{(p)}}\}}{n^{(p)}} \bar{P}_{\text{dir}}^{(p)}, & \text{if } i \neq j \\ 1 - \{1-(1-A_{R^{(p)}})^{n^{(p)}}\} \bar{P}_{\text{dir}}^{(p)}, & \text{otherwise} \end{cases} \tag{9}$$

where

$$\bar{P}_{\text{dir}}^{(p)} \triangleq \frac{2\pi}{A_{R^{(p)}} \vartheta (\frac{N_0 \theta}{\psi^{(p)} \sigma_0^2})^{\frac{2}{\vartheta}}} \int_0^{\frac{N_0 \theta}{\psi^{(p)} \sigma_0^2} (R^{(p)})^{\vartheta}} e^{-t} t^{\frac{2}{\vartheta}-1} dt \tag{10}$$

and

$$A_{R^{(p)}} \triangleq \pi (R^{(p)})^2. \tag{11}$$

If i' and j' are two secondary nodes the expected probability that a class-2 job is forwarded from station

i' to j' is given as,

$$\bar{r}_{i'j'}^{(2,2)} = \begin{cases} \frac{(1-q^{(s)})\{1-(1-A_{R^{(s)}})^{n^{(s)}}\}}{n^{(s)}} \bar{P}_{\text{dir}}^{(s)}, & \text{if } i' \neq j' \\ 1-\{1-(1-A_{R^{(s)}})^{n^{(s)}}\}\bar{P}_{\text{dir}}^{(s)}, & \text{otherwise} \end{cases} \tag{12}$$

where

$$\bar{P}_{\text{dir}}^{(s)} \triangleq \frac{2\pi}{A_{R^{(s)}}\vartheta(\frac{N_0\theta}{\psi^{(s)}\sigma_0^2})^{\frac{2}{\vartheta}}} \int_0^{\frac{N_0\theta}{\psi^{(s)}\sigma_0^2}(R^{(s)})^{\vartheta}} e^{-t} t^{\frac{2}{\vartheta}-1} dt \tag{13}$$

and

$$A_{R^{(s)}} \triangleq \pi(R^{(s)})^2. \tag{14}$$

Proof is provided in [28].

Lemma 2: The arrival rate of class-2 jobs at a primary station i is given as,

$$\lambda_i^{(2)} = \frac{\lambda^{(p)}}{q^{(p)}\bar{P}_{\text{dir}}^{(p)}}, \tag{15}$$

and the arrival rate of class-2 jobs at a secondary station k is given as,

$$\lambda_k^{(2)} = \frac{\lambda^{(s)}}{q^{(s)}\bar{P}_{\text{dir}}^{(s)}}. \tag{16}$$

Proof is provided in [28]. Let $\hat{N}_i^{(p)}$ and $\hat{N}_i^{(s)}$ denote the number of primary and secondary interfering neighbors of node i.

Lemma 3: The average value of $\hat{N}_i^{(p)}$, denoted as $\bar{\hat{N}}_i^{(p)}$ is,

$$\bar{\hat{N}}_i^{(p)} = \begin{cases} 4n^{(p)}\pi(R^{(p)})^2, & \text{if } i \text{ is a primary node} \\ (n^{(p)}+1)\pi(R^{(p)}+R^{(s)})^2, & \text{otherwise} \end{cases} \tag{17}$$

The average value of $\hat{N}_i^{(s)}$, denoted as $\bar{\hat{N}}_i^{(s)}$ is,

$$\bar{\hat{N}}_i^{(s)} = \begin{cases} 0, & \text{if } i \text{ is a primary node} \\ 4n^{(s)}\pi(R^{(s)})^2, & \text{otherwise} \end{cases} \tag{18}$$

Proof is provided in [28]. We assume that the primary and secondary packet generation are Poisson processes even though our analysis can be easily extended to non-Poisson processes as well.

Theorem 1: The average end-to-end delay of a secondary packet, $D(n^{(s)}, n^{(p)})$ is given as

$$D(n^{(s)}, n^{(p)}) = \bar{D}_k \frac{1}{q^{(s)}}, \tag{19}$$

where $\bar{D}_k$ is the average system delay for secondary packets at a secondary node k and is a function of known parameters. The function is closed form except for terms corresponding to probability of successful transmission, $\bar{P}_{\text{dir}}^{(p)}$ and $\bar{P}_{\text{dir}}^{(s)}$ which are obtained from (10) and (13) respectively using numerical integration. The proof is in Appendix A.

V. Delay analysis for cooperative protocol

We derive the expected probability of successful transmission of a primary packet to any relay node, and from a relay node to primary receiver in Lemmas 4 and 5 respectively. In Lemma 6 we find the arrival-rate of class-2 jobs corresponding to primary packets at any secondary station. Theorem 2 follows from Lemmas 4, 5 and 6 along with approximation results from [7] and [8] and characterizes the average end-to-end delay for secondary packets.

Let $P_{\text{rel},(i,j)}^{(p)}$ denote the probability that a packet transmitted by primary node i to its transmission neighbor j enters transmission queue at some relay of (i,j). For any secondary node k let $P[i \to k|(i,j)]$ denote joint probability of the events: "k is a relay of (i,j)" and "packet transmitted by i to j is successfully received at k".

Lemma 4: The mean of $P_{\text{rel},(i,j)}^{(p)}$ is given as,

$$\bar{P}_{\text{rel},(i,j)}^{(p)} = (1-\bar{P}_{\text{dir}}^{(p)})\{1-(1-\bar{P}[i \to k|(i,j)])^{n^{(s)}+1}\}$$

where the expression for $\bar{P}[i \to k|(i,j)]$ is provided in (27).

Given $d_{ij} = z$, the probability that k is a relay of (i,j) is the probability that k is located within distance z from i and less than d_{rel} from j. This is equal to the probability that a secondary node is in the shaded

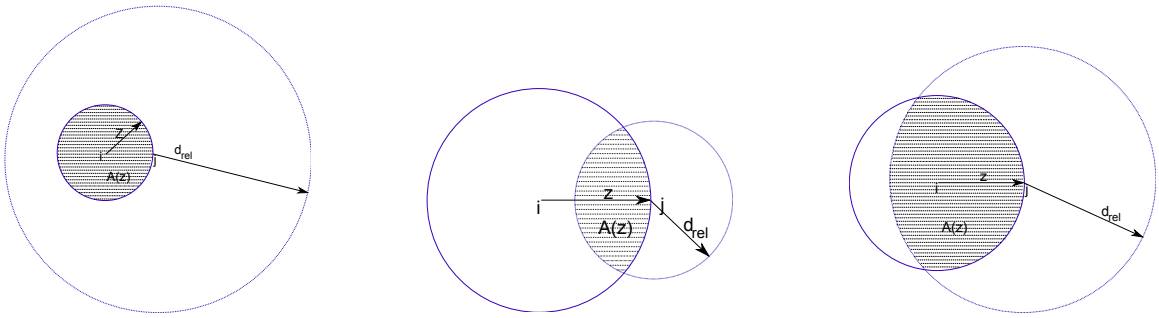

(a) $d_{\text{rel}} \geq 2z$. (b) $d_{\text{rel}} \leq \sqrt{2}z$ (c) $2z > d_{\text{rel}} > \sqrt{2}z$

Fig. 4. Shaded region of area $A(z)$ represents possible locations of a secondary relay for the pair (i, j), where i and j denotes two primary transmission neighbors, as a function of parameter d_{rel} and distance z between i and j.

region shown in Fig. 4. The area of this region, denoted as $A_{\text{rel}}(z)$, is obtained using the formula for finding area of overlapped region of two circles [34] as,

$$A_{\text{rel}}(z) = \begin{cases} \pi z^2, & \text{if } d_{\text{rel}} \geq 2z \\ V_1 + V_2, & \text{if } d_{\text{rel}} \leq \sqrt{2}z \\ V_3 + V_2, & \text{otherwise} \end{cases} \tag{20}$$

where

$$V_1 = z^2 \cos^{-1}(\frac{x}{z}) - x\sqrt{z^2 - x^2} \tag{21}$$

$$V_2 = d_{\text{rel}}^2 \cos^{-1}(\frac{z-x}{d_{\text{rel}}}) - (z-x)\sqrt{d_{\text{rel}}^2 - (z-x)^2} \tag{22}$$

$$V_3 = \pi z^2 - (z^2 \cos^{-1}(\frac{-x}{z}) + x\sqrt{z^2 - x^2}) \tag{23}$$

$$x = z - \frac{d_{\text{rel}}^2}{2z} \tag{24}$$

Let $\Phi_{(i,j),k}$ denote the probability of k being a relay of (i, j). The value of $\Phi_{(i,j),k}$ is obtained by integrating, over all z from 0 to $R^{(p)}$, the product of $A_{\text{rel}}(z)$ and conditional probability of j being on an infinitesimal circular strip of width dz i.e.

$$\Phi_{(i,j),k} = \int_0^{R^{(p)}} A_{\text{rel}}(z) \frac{2\pi z}{A_{R^{(p)}}} dz. \tag{25}$$

From symmetry $\Phi_{(i,j),k}$ is same for all primary transmitter-receiver pairs and secondary nodes. Therefore the index is dropped and we refer to $\Phi_{(i,j),k}$ simply as Φ.

Given $d_{ij} = z$ we denote as v_x and v_y the x and y components, respectively, of any point v in shaded area $A_{\text{rel}}(z)$ with origin of the co-ordinate system being at i. Due to (3) the conditional probability of successful transmission from i to a relay k of (i, j), given j is located on an infinitesimal circular strip of width dz at distance z from i, is $\frac{\iint_{v \in \text{ Area } A_{\text{rel}}(z)} \exp(-\frac{N_0\theta}{\psi^{(p)}\sigma_0^2({v_x}^2+{v_y}^2)^{-\frac{\vartheta}{2}}}) dxdy}{A_{\text{rel}}(z)}$. Therefore $\bar{P}[i \to k|(i,j), k \text{ is a relay of } (i,j)]$ equals $\int_{z=0}^{R^{(p)}} \frac{\iint_{v \in \text{ Area } A_{\text{rel}}(z)} \exp(-\frac{N_0\theta}{\psi^{(p)}\sigma_0^2({v_x}^2+{v_y}^2)^{-\frac{\vartheta}{2}}}) dxdy}{A_{\text{rel}}(z)} \frac{2\pi z}{A_{R^{(p)}}} dz$.

The expected value of $P[i \to k|(i,j)]$ is,

$$\bar{P}[i \to k|(i,j)] = \bar{P}[i \to k|(i,j), k \text{ is a relay of } (i,j)] .P[k \text{ is a relay of}(i,j)] \tag{26}$$

$$= \Phi \int_{z=0}^{R^{(p)}} \frac{\iint_{v \in \text{ Area } A_{\text{rel}}(z)} \exp(-\frac{N_0\theta}{\psi^{(p)}\sigma_0^2({v_x}^2+{v_y}^2)^{-\frac{\vartheta}{2}}}) dxdy 2\pi z}{A_{\text{rel}}(z) A_{R^{(p)}}} dz \tag{27}$$

Note that $\bar{P}[i \to k|(i,j)]$ is same for all (i, j) and k due to symmetry of primary and secondary nodes. Now $P_{\text{rel},(i,j)}^{(p)}$ is the joint probability of the events: "transmission from i to j is unsuccessful" and " transmission from i to at least one of the relays of (i, j) is successful". Since those two events are independent, the

average value of $P^{(p)}_{\text{rel},(i,j)}$ is therefore,

$$\bar{P}^{(p)}_{\text{rel},(i,j)} = (1-\bar{P}^{(p)}_{\text{dir}})\{1-(1-\bar{P}[i\rightarrow k|(i,j)])^{n^{(s)}+1}\} \tag{28}$$

Due to symmetry of primary nodes, $\bar{P}^{(p)}_{\text{rel},(i,j)}$ is equal for all (i,j) and hence-forth we refer to $\bar{P}^{(p)}_{\text{rel},(i,j)}$ simply as $\bar{P}^{(p)}_{\text{rel}}$. Let $P^{(s)}_{\text{rel},(i,j),k}$ denote the probability of successful transmission of a primary packet from a relay k of (i,j) to j.

Lemma 5: The mean of $P^{(s)}_{\text{rel},(i,j),k}$ is given as,

$$\bar{P}^{(s)}_{\text{rel},(i,j),k} = \int_0^{R^{(p)}} \frac{\iint_{v\in \text{ Area } A_{\text{rel}}(z)} \exp(-\frac{N_0\theta}{\psi^{(p)}\sigma_0^2\{(v_x-z)^2+{v_y}^2\}^{-\frac{\vartheta}{2}}})dxdy2\pi z}{A_{\text{rel}}(z)A_{R^{(p)}}}dz$$

Proof is provided in [28]. Due to the symmetry of primary and secondary nodes, $\bar{P}^{(s)}_{\text{rel},(i,j),k}$ is equal for all (i,j) and k. Hence-forth we refer to $\bar{P}^{(s)}_{\text{rel},(i,j),k}$ simply as $\bar{P}^{(s)}_{\text{rel}}$.

Lemma 6: The arrival rate of class-2 jobs corresponding to primary packets at any secondary station, denoted as λ_{ext}, is given as,

$$\lambda_{\text{ext}} = \frac{\lambda^{(p)}\bar{P}^{(p)}_{\text{rel}}(n^{(p)}+1)}{\bar{P}^{(p)}_{\text{coop}}q^{(p)}(n^{(s)}+1)\bar{P}^{(s)}_{\text{rel}}} \tag{29}$$

where

$$\bar{P}^{(p)}_{\text{coop}} = \bar{P}^{(p)}_{\text{rel}} + \bar{P}^{(p)}_{\text{dir}} \tag{30}$$

Proof is provided in [28].

Theorem 2: Under the cooperative protocol, the average end-to-end delay of a secondary packet, $D(n^{(s)},n^{(p)})$ is given as

$$D(n^{(s)},n^{(p)}) = \bar{D}_k\frac{1}{q^{(s)}}, \tag{31}$$

where $\bar{D}_k$ is the average system delay for secondary packets at a secondary node k and is a function of known parameters. The function is closed form except for the terms corresponding to probability of successful transmission: $\bar{P}^{(p)}_{\text{coop}}$, $\bar{P}^{(s)}_{\text{rel}}$ and $\bar{P}^{(s)}_{\text{dir}}$ which are obtained from (30), (29) and (13) respectively using numerical integration.

The proof is similar to that of Theorem 1 in Section IV except for the following difference: the average routing probability between primary and secondary stations is non-zero due to cooperation. Detailed proof is provided in [28].

VI. Maximum achievable throughput

In this section we investigate under what conditions cooperation improves the throughput of primary and secondary users. We compare the maximum achievable throughput of primary and secondary users both with and without cooperation using the priority queuing network representation. The maximum achievable throughput of secondary users, for a given primary packet generation rate $\lambda^{(p)}$, is defined as the maximum packet generation rate $\lambda^{(s)}$ for which the queue-length at every secondary node remains bounded. In the rest of this section we assume $n^{(p)}$ and $n^{(s)}$ are sufficiently large such that $n^{(p)}+1\approx n^{(p)}$ and $n^{(s)}+1\approx n^{(s)}$.

Corrolary 1: Under the cooperative protocol the maximum achievable throughput for secondary users with cooperation, denoted as $\lambda^{(s)}_{\text{max,coop}}(\lambda^{(p)})$, corresponding to primary packet generation rate $\lambda^{(p)}$ is,

$$\lambda^{(s)}_{\text{max,coop}}(\lambda^{(p)}) = \max\{T_A - T_B - T_C, 0\} \tag{32}$$

where $T_A = \frac{q^{(s)}\bar{P}^{(s)}_{\text{dir}}}{\frac{L}{W}+\frac{1}{\xi}+\frac{L}{W}\tilde{\hat{N}}^{(s)}_i}$, $T_B = \frac{\hat{N}^{(p)}_i L\lambda^{(p)}q^{(s)}\bar{P}^{(s)}_{\text{dir}}}{Wq^{(p)}\bar{P}^{(p)}_{\text{coop}}(\frac{L}{W}+\frac{1}{\xi}+\frac{L}{W}\hat{\tilde{N}}^{(s)}_i)}$ and $T_C = \frac{q^{(s)}\bar{P}^{(s)}_{\text{dir}}\lambda^{(p)}\bar{P}^{(p)}_{\text{rel}}n^{(p)}}{n^{(s)}\bar{P}^{(s)}_{\text{rel}}q^{(p)}\bar{P}^{(p)}_{\text{coop}}}$.

Proof is provided in [28]. The first term T_A in the right hand side (RHS) of (32) is the maximum throughput for secondary users in absence of any primary traffic. The second term T_B in the RHS of (32) corresponds to reduction in throughput of a secondary node due to packet transmission from primary interfering neighbors. The third term T_C corresponds to reduction in throughput of a secondary node due to primary packet transmission from secondary interfering neighbors.

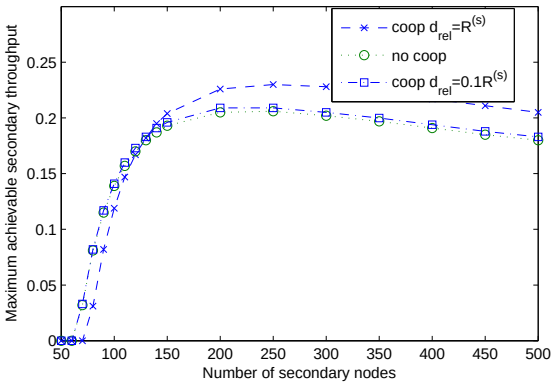

Fig. 5. Comparison of maximum achievable throughput of secondary nodes with cooperation vs non-cooperation for two values of d_{rel}: $R^{(s)}$ and $0.1R^{(s)}$. Value of $n^{(p)}$ is 100 and $\lambda^{(p)}$ is 0.8725, the maximum achievable throughput for primary users without cooperation.

Comparison of Maximum Achievable Throughput With and Without Cooperation

For the non-cooperative protocol, the maximum achievable throughput for secondary users, for a given $\lambda^{(p)}$ is obtained from (32) by replacing $\bar{P}^{(p)}_{\text{coop}}$ and $\bar{P}^{(p)}_{\text{rel}}$ with $\bar{P}^{(p)}_{\text{dir}}$ and 0 respectively. We denote this term as $\lambda^{(s)}_{\text{max,non-coop}}(\lambda^{(p)})$ whose expression is given as

$$\lambda^{(s)}_{\text{max,non-coop}}(\lambda^{(p)}) = \max\{T_A - T_D, 0\} \tag{33}$$

where

$$T_D = \frac{\bar{\hat{N}}^{(p)}_i L\lambda^{(p)} q^{(s)} \bar{P}^{(s)}_{\text{dir}}}{W q^{(p)} \bar{P}^{(p)}_{\text{dir}} (\frac{L}{W} + \frac{1}{\xi} + \frac{L}{W}\bar{\hat{N}}^{(s)}_i)} \tag{34}$$

Let $\lambda^{(p)}_{\text{max,non-coop}}$ denote the maximum achievable throughput for primary nodes without cooperation. Clearly, $\lambda^{(p)}_{\text{max,non-coop}}$ can be obtained by calculating $\lambda^{(s)}_{\text{max,non-coop}}(0)$ for a secondary network with its parameters same as that of the primary network. Hence,

$$\lambda^{(p)}_{\text{max,non-coop}} = \frac{q^{(p)} \bar{P}^{(p)}_{\text{dir}}}{\frac{L}{W} + \frac{1}{\xi} + \frac{L}{W}\bar{\hat{N}}^{(p)}_i} \tag{35}$$

From (32) and (33) we observe $\lambda^{(s)}_{\text{max,coop}}(\lambda^{(p)})$ and $\lambda^{(s)}_{\text{max,non-coop}}(\lambda^{(p)})$ decrease linearly with increasing $\lambda^{(p)}$ until they become zero. Hence, the maximum achievable throughput of secondary users with cooperation is higher than that without cooperation if

$$T_A - T_D \leq T_A - T_B - T_C \text{ i.e.,}$$

$$\frac{\bar{\hat{N}}^{(p)}_i L q^{(s)} \bar{P}^{(s)}_{\text{dir}}}{W q^{(p)} \bar{P}^{(p)}_{\text{coop}} (\frac{L}{W} + \frac{1}{\xi} + \frac{L}{W}\bar{\hat{N}}^{(s)}_i)} + \frac{q^{(s)} \bar{P}^{(s)}_{\text{dir}} \bar{P}^{(p)}_{\text{rel}} n^{(p)}}{n^{(s)} \bar{P}^{(s)}_{\text{rel}} q^{(p)} \bar{P}^{(p)}_{\text{coop}}}$$

$$\leq \frac{\bar{\hat{N}}^{(p)}_i L q^{(s)} \bar{P}^{(s)}_{\text{dir}}}{W q^{(p)} \bar{P}^{(p)}_{\text{dir}} (\frac{L}{W} + \frac{1}{\xi} + \frac{L}{W}\bar{\hat{N}}^{(s)}_i)}. \tag{36}$$

Next we compare the throughput of primary users with and without cooperation. The maximum achievable throughput of primary nodes with cooperation for a given $\lambda^{(s)}$, denoted as $\lambda^{(p)}_{\text{max,coop}}(\lambda^{(s)})$, is the maximum value of $\lambda^{(p)}$ for which the transmission queue of both primary and secondary nodes are stable. The maximum value of $\lambda^{(p)}$ for which the transmission queue of primary nodes are stable is obtained by replacing $\bar{P}^{(p)}_{\text{dir}}$ with $\bar{P}^{(p)}_{\text{coop}}$ in (35) as

$$T_1 = \frac{q^{(p)} \bar{P}^{(p)}_{\text{coop}}}{\frac{L}{W} + \frac{1}{\xi} + \frac{L}{W}\bar{\hat{N}}^{(p)}_i} \tag{37}$$

The maximum value of $\lambda^{(p)}$ for which the transmission queue of secondary nodes are stable is obtained similar to the calculations in the proof of Corollary 1 as

$$T_2(\lambda^{(s)}) = \max\{T_E - T_F - T_G, 0\} \tag{38}$$

where $T_E = \frac{\mu_i^{(2)}}{H_2+(H_3+\bar{\tilde{N}}^{(s)}H_2)\frac{\mu_i^{(2)}}{\mu_i^{(1)}}}$, $T_F = \frac{\lambda^{(s)}H_1}{H_2+(H_3+\bar{\tilde{N}}^{(s)}H_2)\frac{\mu_i^{(2)}}{\mu_i^{(1)}}}$ and $T_G = \frac{\frac{\lambda^{(s)}H_1\bar{\tilde{N}}_i^{(s)}\mu_i^{(2)}}{\mu_i^{(1)}}}{H_2+(H_3+\bar{\tilde{N}}^{(s)}H_2)\frac{\mu_i^{(2)}}{\mu_i^{(1)}}}$. The terms H_1, H_2, H_3 are defined in [28]. Therefore, cooperation benefits primary users for a given $\lambda^{(s)}$ if

$$\lambda^{(p)}_{\text{max,coop}}(\lambda^{(s)}) = \min(T_2(\lambda^{(s)}), T_1) > \frac{q^{(p)}\bar{P}^{(p)}_{\text{dir}}}{\frac{L}{W}+\frac{1}{\xi}+\frac{L}{W}\bar{\tilde{N}}_i^{(p)}} \tag{39}$$

Example: We use a numerical example to illustrate how $\lambda^{(s)}_{\text{max,coop}}$ varies with number of secondary users. In Fig 5 we plot $\lambda^{(s)}_{\text{max,coop}}(\lambda^{(p)}_{\text{max,noncoop}})$, $\lambda^{(s)}_{\text{max,noncoop}}(\lambda^{(p)}_{\text{max,noncoop}})$ when $n^{(p)}$ is 100 and $n^{(s)}$ varies from 50 to 500. ϑ equals 2; the parameters N_0, θ, $\psi^{(p)}$ and $\psi^{(s)}$ are selected such that $\bar{P}^{(p)}_{\text{dir}} = \bar{P}^{(s)}_{\text{dir}} = 0.7$. $R^{(p)}$, $R^{(s)}$, $q^{(p)}$, $q^{(s)}$, W and L are selected as $\sqrt{\frac{log(n^{(p)})}{n^{(p)}}}$, $\sqrt{\frac{log(n^{(s)})}{n^{(s)}}}$, $0.4R^{(p)}$, $0.4R^{(s)}$, 10^6 bits/sec and 1000 respectively. We select $R^{(p)}$, $R^{(s)}$, $q^{(p)}$ and $q^{(s)}$ to make the average number of hops and transmission range comparable to that in [29][8].

$\lambda^{(p)}_{\text{max,noncoop}}$ is found to be 0.8725. Two different values of d_{rel}: $R^{(s)}$ and $0.1R^{(s)}$ are used.
In Fig 5 when d_{rel} is $R^{(s)}$, cooperation reduces throughput for secondary users when $n^{(s)}$ is lower than about 120. At this range the distance between relay nodes and primary receivers is somewhat large which leads to a small probability of successful transmission from relay node to corresponding primary receiver. Any gain in transmission opportunities for secondary nodes due to lower transmission from primary interfering neighbors is offset by interference due to high transmission attempts of primary packets by secondary interfering neighbors. As $n^{(s)}$ increases d_{rel} becomes progressively lower and $\bar{P}^{(s)}_{\text{rel}}$ is high because relay nodes are closer to corresponding primary receivers. Therefore the maximum achievable throughput of secondary users increases with cooperation at higher $n^{(s)}$.
In Fig 5 when d_{rel} is $0.1R^{(s)}$ cooperation does not hurt at low $n^{(s)}$ because the distance from relay nodes to primary receivers is small. However the gain due to cooperation is small at high $n^{(s)}$ as compared to the case of $d_{\text{rel}} = R^{(s)}$. This is because, due to small d_{rel}, there are fewer relay nodes per primary transmitter-receiver pair and the network is close to the case without cooperation.

For this choice of network parameters we observe in Fig 5 that the maximum achievable throughput, with or without cooperation, first increases with $n^{(s)}$ and then decreases. This is because $\lambda^{(s)}_{\text{max,coop}}$ decreases with increasing average number of interfering neighbors to a secondary node. The average number of primary and secondary interfering neighbors decrease and increase respectively with increasing $n^{(s)}$, when $R^{(s)} = \sqrt{\frac{log(n^{(s)})}{n^{(s)}}}$. The former effect is dominant at low $n^{(s)}$; the latter effect is dominant at high $n^{(s)}$.

Next we use a numerical example to illustrate how cooperation can improve primary user throughput. In Fig 6 we plot $\lambda^{(p)}_{\text{max,coop}}(\lambda^{(s)})$ when $n^{(p)}$ is 100, $n^{(s)}$ varies from 50 to 500. For each value of $n^{(s)}$, we select $\lambda^{(s)}$ as the maximum achievable throughput for secondary users without cooperation when $\lambda^{(p)}$ is 0.8725 i.e., $\lambda^{(s)} = \lambda^{(s)}_{\text{max,noncoop}}(\lambda^{(p)}_{\text{max,noncoop}})$. We select $d_{\text{rel}} = R^{(s)}$; other parameters remain the same as used in Fig 5. We observe, cooperation reduces throughput for primary users when $n^{(s)}$ is lower than about 120 similar to what observed in Fig 5 because of small probability of successful transmission from relay node to corresponding primary receiver. Throughput of primary user increases at higher $n^{(s)}$ because $\bar{P}^{(s)}_{\text{rel}}$ is high at those values.

VII. Simulations

We compare our analytical results with those obtained through simulation in C-programming language so as to verify the validity of our assumptions. The simulation setting consists of $n^{(p)}+1$ primary and $n^{(s)}+1$ secondary nodes that are uniformly distributed over the surface of a torus of unit area. The length of

[8]According to [29] the expected distance between a source-destination pair in a homogeneous network of n nodes is constant and transmission range of a node is $\omega(\sqrt{logn/n})$. Therefore, the expected number of hops in every source-destination pair is $o(\sqrt{n/logn})$. The expected number of hops for a primary (respectively secondary) source-destination pair in our model, obtained as part of the proof of Theorem 1, is $\frac{1}{q^{(p)}}$ (resp. $\frac{1}{q^{(s)}}$). Therefore, for comparable parameters as in [29], we select $R^{(p)} = \sqrt{\frac{log(n^{(p)})}{n^{(p)}}}$, $R^{(s)} = \sqrt{\frac{log(n^{(s)})}{n^{(s)}}}$ $q^{(p)} = 0.4R^{(p)}$, $q^{(s)} = 0.4R^{(s)}$.

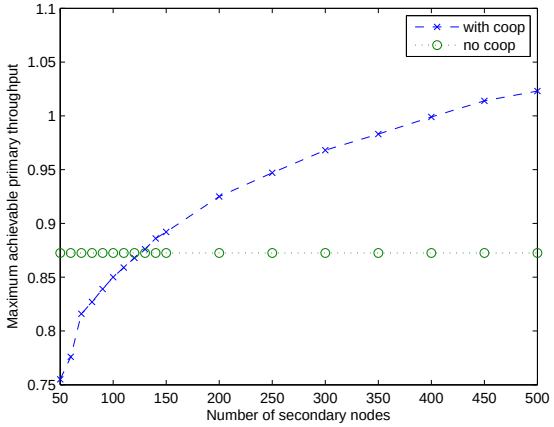

Fig. 6. Comparison of maximum achievable throughput of primary nodes with cooperation vs non-cooperation for $d_{\text{rel}} = R^{(s)}$. Value of $n^{(p)}$ is 100; $\lambda^{(s)}$ is the maximum achievable throughput for secondary users without cooperation when $\lambda^{(p)}$ is 0.8725, the maximum achievable throughput for primary users without cooperation.

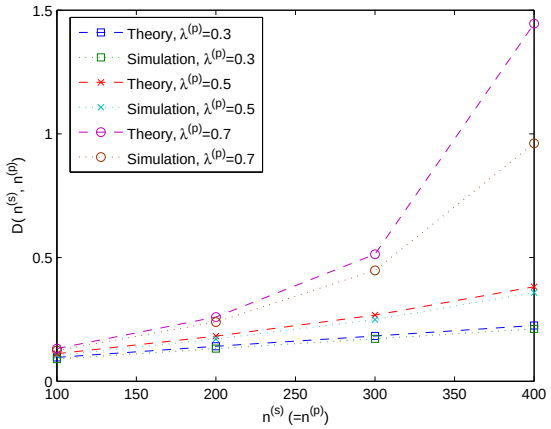

(a) Average end-to-end delay of secondary packets versus number of primary (= number of secondary) nodes.

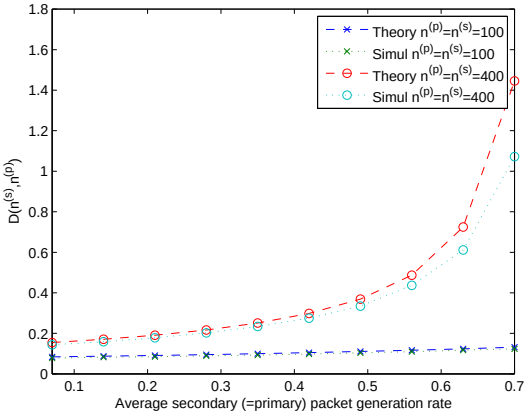

(b) Average end-to-end delay of secondary packets versus secondary (= primary) packet generation rate.

Fig. 7. Comparison of the analytical and simulation results without cooperation.

a primary or a secondary packet is 1KB. The transmission rate (W) of the channel is 10^6 bits/sec. The back-off timers for both primary and secondary nodes are exponentially distributed with mean back-off duration of 0.01 seconds. We average simulation results over 20 different randomly generated topologies. Each topology is selected such that the average number of interfering neighbors to every primary and secondary node is within a small number, selected as 0.7, from their respective theoretical values. The simulation uses probabilistic routing scheme as described in Section II. N_0, σ_0 and θ are fixed while $\psi^{(p)}$ and $\psi^{(s)}$ are varied such that $\bar{P}_{\text{dir}}^{(p)} = \bar{P}_{\text{dir}}^{(s)} = 0.7$ for every combination of $n^{(s)}$ and $n^{(p)}$. Each packet transmission from a primary node to its transmission neighbor is successful with probability $\bar{P}_{\text{dir}}^{(p)}$; otherwise (in case of cooperation) it is forwarded to one of the secondary relays with probability $\frac{\bar{P}_{\text{rel}}^{(p)}}{\{1-(1-\Phi)^{n^{(s)}+1}\}(1-\bar{P}_{\text{dir}}^{(p)})}$. The term $\frac{\bar{P}_{\text{rel}}^{(p)}}{\{1-(1-\Phi)^{n^{(s)}+1}\}(1-\bar{P}_{\text{dir}}^{(p)})}$ is the theoretical average probability of successful transmission from a primary node to relay, given direct transmission from primary node fails and at least one such relay exists for the corresponding primary transmission neighbor pair. Each secondary packet transmission from a secondary node to its transmission neighbor is successful with probability $\bar{P}_{\text{dir}}^{(s)}$. Each primary packet transmission from a secondary node is successful with probability $\bar{P}_{\text{rel}}^{(s)}$. Each simulation is run for 1000 seconds.

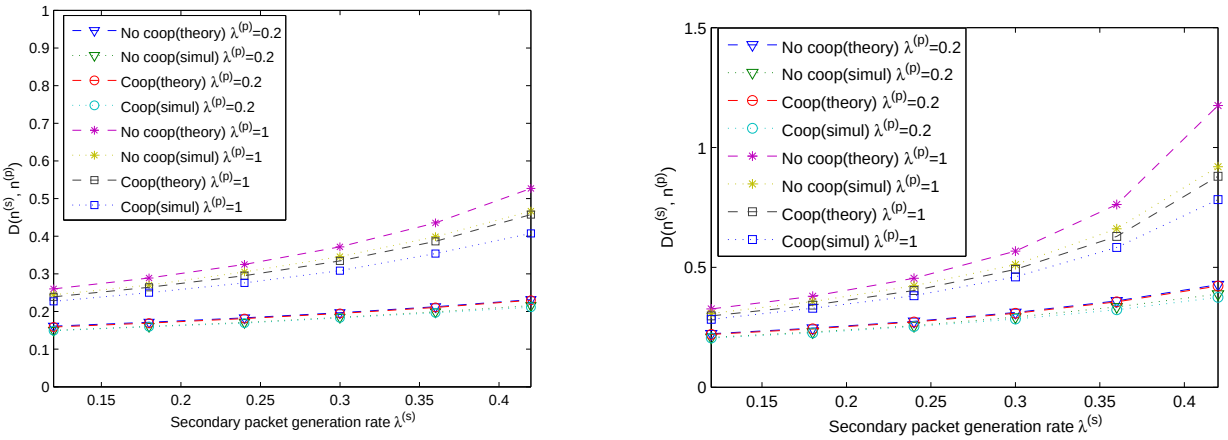

(a) $n^{(s)}$ equals 200. (b) $n^{(s)}$ equals 400.

Fig. 8. Plot of average delay of secondary packets vs packet generation-rates with and without cooperation when $n^{(p)}$ equals 100.

A. Simulations for Non-cooperative Protocol

For Fig 7a and Fig 7b $R^{(p)}$ and $R^{(s)}$ are chosen as $0.8\sqrt{\frac{log(n^{(p)})}{n^{(p)}}}$ and $0.8\sqrt{\frac{log(n^{(s)})}{n^{(s)}}}$ respectively. For both figures $q^{(p)}$ and $q^{(s)}$ are chosen as $\sqrt{\frac{log(n^{(p)})}{n^{(p)}}}$ and $\sqrt{\frac{log(n^{(s)})}{n^{(s)}}}$ respectively.

In Fig. 7a, we plot the average end-to-end delay for three values of $\lambda^{(s)} = \lambda^{(p)}$: 0.3, 0.5 and 0.7 respectively while $n^{(s)}(= n^{(p)})$ is varied from 100 to 400 at steps of 100. Fig. 7b shows the average end-to-end delay when $n^{(s)} = n^{(p)}$= 100 and 400, while $\lambda^{(s)}(= \lambda^{(p)})$ is varied from 0.07 to 0.7. As expected the average end-to-end delay monotonically increases with increasing number of nodes and traffic generation rate in both figures.

Channel utilization of a secondary node i is the fraction of time the channel local to a node is not idle (i.e. either the given node or any of its interfering neighbors is transmitting). This is equal to $\frac{\lambda_i^{(1)} L}{W}$. We observe that the network model is reasonably accurate for a wide range of channel utilization of a secondary node (an increasing function of $\lambda^{(s)}$ and $\lambda^{(p)}$) except for high range. In Fig. 7a, the channel utilization is about 0.63 when $\lambda^{(s)} = 0.7$ and $n^{(s)} = 300$. A similar result is observed from Fig. 7b. For higher channel utilization scenarios, our approximation of the arrival process of class-1 jobs at any station as sum of individual transmission processes is no longer accurate as there are significant number of instances when two or more interfering neighbors of any node are simultaneously transmitting. In this case, our approximation leads to over-estimating the duration of such interruptions and the theoretical average end-to-end delay acts as an upper bound to that obtained from simulation results.

B. Simulations for Cooperative Protocol

In Fig. 8a and Fig. 8b, we compare the average end-to-end delay, from theory and simulation, under cooperation with $n^{(p)}$ as 100 and $n^{(s)}$ as 200 and 400 respectively. Two values of $\lambda^{(p)}$: 0.2 and 1 are used; $\lambda^{(s)}$ is varied from 0.06 to 0.42 in steps of 0.06. In both figures $R^{(p)}$, $R^{(s)}$, $q^{(p)}$ and $q^{(s)}$ are selected as $\sqrt{\frac{log(n^{(p)})}{n^{(p)}}}$, $\sqrt{\frac{log(n^{(s)})}{n^{(s)}}}$, $0.8R^{(p)}$ and $0.8R^{(s)}$ respectively. In order to observe the performance gain due to cooperation we also plot the corresponding average end-to-end delay, both from theory and simulation, without cooperation.

We observe that secondary users benefit from cooperation, reflected in lower average delay with cooperation in both figures. The benefit is small for lower $\lambda^{(p)}$; average delay with and without cooperation are almost the same when $\lambda^{(p)}$ is 0.2. It is more pronounced for higher $\lambda^{(p)}$ as can be observed from both figures when $\lambda^{(p)}$ is 1.

Like in Fig. 7 and for same reasons, the theory and simulation in Fig. 8 matches well when the channel utilization is low and vary at high channel utilizations. For example, the theory and simulation results match when $\lambda^{(p)}$ is 0.2. In Fig. 8b, the theory and simulation results for the non-cooperative case begin to vary when $\lambda^{(p)} = 1$ and $\lambda^{(s)} \geq 0.3$; the channel utilization at $\lambda^{(p)} = 1, \lambda^{(s)} = 0.3$ is 0.63.

VIII. Conclusions

In this paper we considered two multi-hop ad-hoc networks using random access based MAC protocol similar to IEEE 802.11, with each network having different priority of channel access. Assuming simple probabilistic routing protocol and a distributed MAC with exponential backoff, we obtained expressions for the average end-to-end delay for the lower priority secondary network under both cooperative and non-cooperative protocols. We verified that our theoretical results match with the simulation results for low to moderate channel utilizations which are the typical operating regions for random MAC protocols. Possible avenues for future work include the extension of the analysis to the case of multiple channels and the modeling of non-ideal channel sensing.

Appendix A
Proof of Theorem 1

We first obtain the average number of jobs at a secondary station in the single-class G/G/1 queuing network representation using (4). This in turn requires knowledge of mean and coefficient of variation of effective service time of jobs in this network. Recall, jobs in the single-class G/G/1 queuing network correspond to class-2 jobs in equivalent 2-class priority queuing network representation. Therefore, we first obtain mean and coefficient of variation of completion time of class-2 jobs at any secondary station in the priority queuing network.

A. Mean Completion Time of Class-2 Jobs at a Secondary Station:

The mean of service time of a class-1 job ($b_i^{(1)}$) at station (primary or secondary) i is given by

$$E[b_i^{(1)}] = \frac{L}{W} = \frac{1}{\mu_i^{(1)}} \tag{40}$$

The mean and second moment of service time of a class-2 job ($b_i^{(2)}$) at i is given by

$$E[b_i^{(2)}] = \frac{1}{\xi} + \frac{L}{W} = \frac{1}{\mu_i^{(2)}} \tag{41}$$

$$E[b_i^{(2)^2}] = \frac{2}{\xi^2} + \frac{L^2}{W^2} + 2\frac{L}{W\xi}. \tag{42}$$

Due to symmetry of primary and secondary nodes, the mean, second-moment and coefficient of variation of inter-arrival time, inter-departure time, completion time for class-1 and class-2 jobs are same for any two primary nodes and for any two secondary nodes.

Let $\hat{M}_{i,k_1}^{(p)}$ and $\hat{M}_{i,k_2}^{(s)}$ denote the k_1-th (where $k_1 = 1, \ldots, \hat{N}_i^{(p)}$) and k_2-th (where $k_2 = 1, \ldots, \hat{N}_i^{(s)}$) primary and secondary interfering neighbor of i respectively. Let $a_i^{(k)}$ denote the inter-arrival time of a class-k (where k=1,2) job at i. We approximate the number of arrival of class-1 jobs at i in time-interval t as being normally distributed with mean $\lambda_i^{(1)}t$ and coefficient of variation of inter-arrival times $C_{Ai}^{(1)}$ where $\lambda_i^{(1)}$ is obtained using (10) from [28] and symmetry property of primary and secondary nodes as,

$$\lambda_i^{(1)} = \bar{\hat{N}}_i^{(p)} \lambda^{(2)}_{\hat{M}_{i,k_1}^{(p)}} + \hat{N}_i^{(s)} \lambda^{(2)}_{\hat{M}_{i,k_2}^{(s)}} \tag{43}$$

and $C_{Ai}^{(1)^2}$ is obtained using (8) as

$$\begin{aligned} C_{Ai}^{(1)^2} = \frac{1}{\lambda_i^{(1)}} \{ & \bar{\hat{N}}_i^{(p)} \lambda^{(2)}_{\hat{M}_{i,k_1}^{(p)}} C^{(2)^2}_{D\hat{M}_{i,k_1}^{(p)}} \\ & + \bar{\hat{N}}_i^{(s)} \lambda^{(2)}_{\hat{M}_{i,k_2}^{(s)}} C^{(2)^2}_{D\hat{M}_{i,k_2}^{(s)}} \} \end{aligned} \tag{44}$$

$C_{Dj}^{(k)}$ denotes the coefficient of variation of interdeparture time of class-k jobs at station j. Let $\gamma_i^{(k-1)}$ denote the duration of a break in service time of a class-k job at station i due to arrival of high priority jobs. Using (15) and (16) from [28] we obtain,

$$E[\gamma_i^{(1)}] = -\frac{1}{\beta_i^{(1)}} \text{ and} \tag{45}$$

$$E[\gamma_i^{(1)^2}] = -\frac{\alpha_i^{(1)}}{\beta_i^{(1)^3}} + \frac{1}{\beta_i^{(1)^2}} \tag{46}$$

where

$$\beta_i^{(1)} = \lambda_i^{(1)} - \mu_i^{(1)} \tag{47}$$

$$\alpha_i^{(1)} = \lambda_i^{(1)}(C_{Ai}^{(1)^2}). \tag{48}$$

The mean of the completion time of a class-2 job at i, $c_i^{(2)}$, is obtained using (5) as,

$$E[c_i^{(2)}] = \{\frac{1}{1-\frac{\lambda_i^{(1)}}{\mu_i^{(1)}}}\}\frac{1}{\mu_i^{(2)}} \tag{49}$$

B. Coefficient of Variation of Completion Time of Class-2 Jobs at a Secondary Station:

Using (5) and (46), the expression of second moment of $c_i^{(2)}$ is given as,

$$\begin{aligned} E[c_i^{(2)^2}] &= E[b_i^{(2)^2}](1+E[\gamma_i^{(1)}]\lambda_i^{(1)})^2 \\ &\quad +E[b_i^{(2)}]\{(E[\gamma_i^{(1)}])^2 C_{Ai}^{(1)^2}\lambda_i^{(1)} \\ &\quad -\lambda_i^{(1)}(E[\gamma_i^{(1)}])^2 + E[\gamma_i^{(1)^2}]\lambda_i^{(1)}\} \\ &= U_{i,1} + U_{i,2}C_{Ai}^{(1)^2} \end{aligned} \tag{50}$$

where

$$\begin{aligned} U_{i,1} &= E[b_i^{(2)^2}](1+E[\gamma_i^{(1)}]\lambda_i^{(1)})^2 \\ &\quad +E[b_i^{(2)}]\{-\lambda_i^{(1)}(E[\gamma_i^{(1)}])^2 + \frac{\lambda_i^{(1)}}{\beta_i^{(1)^2}}\} \end{aligned} \tag{51}$$

$$U_{i,2} = E[b_i^{(2)}](E[\gamma_i^{(1)}])^2\lambda_i^{(1)} - \frac{(\lambda_i^{(1)})^2 E[b_i^{(2)}]}{\beta_i^{(1)^3}} \tag{52}$$

The unknown variable $C_{Ai}^{(1)^2}$ in (50) is obtained by solving 8 linear equations in 8 unknowns: squared coefficient of variation of inter-arrival time of class-1 jobs at any primary and secondary station (denoted as $C_{A,p}^{(1)^2}$ and $C_{A,s}^{(1)^2}$), squared coefficient of variation of inter-arrival time of class-2 jobs at any primary and secondary station (denoted as $C_{A,p}^{(2)^2}$ and $C_{A,s}^{(2)^2}$), squared coefficient of variation of inter-departure time of class-2 jobs at any primary and secondary station (denoted as $C_{D,p}^{(2)^2}$ and $C_{D,s}^{(2)^2}$), and second moment of inter-departure time of class-2 jobs at any primary (denoted as $f_p^{(2)}$) and secondary station (denoted as $f_s^{(2)}$). Next, we establish those equations.

We first obtain mean and second moment of the inter-departure time of a class-2 job at i, $f_i^{(2)}$. From (7), the mean of $f_i^{(2)}$ is obtained as,

$$\begin{aligned} E[f_i^{(2)}] &= E[c_i^{(2)}] + (1-\frac{\rho_i^{(2)}}{1-\rho_i^{(1)}})(E[a_i^{(2)}]) \\ &\quad +\rho_i^{(1)}(1-\frac{\rho_i^{(2)}}{1-\rho_i^{(1)}})E[\gamma_i^{(1)}], \end{aligned} \tag{53}$$

where

$$\rho_i^{(k)} = \frac{\lambda_i^{(k)}}{\mu_i^{(k)}} \quad \forall k = 1,2 \text{ and} \tag{54}$$

$$E[a_i^{(2)}] = \frac{1}{\lambda_i^{(2)}}. \tag{55}$$

From (7) the second moment of $f_i^{(2)}$ is obtained as,

$$\begin{aligned} E[{f_i^{(2)}}^2] &= E[{c_i^{(2)}}^2] + (1 - \frac{\rho_i^{(2)}}{1-\rho_i^{(1)}})(E[{a_i^{(2)}}^2] \\ &\quad +2E[c_i^{(2)}]E[a_i^{(2)}]) \\ &\quad +\rho_i^{(1)}(1 - \frac{\rho_i^{(2)}}{1-\rho_i^{(1)}})\{E[{\gamma_i^{(1)}}^2] \\ &\quad +2E[\gamma_i^{(1)}](E[c_i^{(2)}] + E[a_i^{(2)}])\} \end{aligned} \tag{56}$$

The squared coefficient of variation of inter-departure times of class-2 jobs at i is,

$$C_{Di}^{(2)^2} = \frac{E[{f_i^{(2)}}^2]}{(E[f_i^{(2)}])^2} - 1 \tag{57}$$

Using the symmetric property and substituting expressions of $E[{\gamma_i^{(1)}}^2]$ and $E[{c_i^{(2)}}^2]$ from (46) and (50) respectively in (56), we have,

$$E[{f_i^{(2)}}^2] = U_{i,3} + U_{i,4}C_{Ai}^{(1)^2} + U_{i,5}C_{Ai}^{(2)^2} \tag{58}$$

where

$$\begin{aligned} U_{i,3} &= U_{i,1} + (1 - \frac{\rho_i^{(2)}}{1-\rho_i^{(1)}})(2E[c_i^{(2)}]E[a_i^{(2)}] + \frac{1}{{\lambda_i^{(2)}}^2}) \\ &\quad +\rho_i^{(1)}(1 - \frac{\rho_i^{(2)}}{1-\rho_i^{(1)}})\{\frac{1}{{\beta_i^{(1)}}^2} \\ &\quad +2E[\gamma_i^{(1)}](E[c_i^{(2)}] + E[a_i^{(2)}])\} \end{aligned} \tag{59}$$

$$U_{i,4} = U_{i,2} - \frac{\lambda_i^{(1)}\rho_i^{(1)}(1 - \frac{\rho_i^{(2)}}{1-\rho_i^{(1)}})}{{\beta_i^{(1)}}^3} \tag{60}$$

$$U_{i,5} = \frac{(1 - \frac{\rho_i^{(2)}}{1-\rho_i^{(1)}})}{{\lambda_i^{(2)}}^2} \tag{61}$$

Now we apply the diffusion approximation from [8] to a network of G/G/1 queues where the inter-arrival time, service time and inter-departure time of jobs from station i are equal to the random variables $a_i^{(2)}$, $c_i^{(2)}$ and $f_i^{(2)}$ respectively. Then using (8) from [28] we obtain

$$\begin{aligned} &C_{Ai}^{(2)^2} = 1 \\ &+ \sum_{j=1}^{n^{(s)}+n^{(p)}+2} \{\frac{E[{c_j^{(2)}}^2] - (E[c_j^{(2)}])^2}{(E[c_j^{(2)}])^2} - 1\}{\bar{r}_{ji}^{(2,2)}}^2 e_j e_i^{-1} \end{aligned} \tag{62}$$

where e_i denotes the mean number of visits of a class-2 job to station i. Let $\tilde{i} \neq i$ denote a node of same type as i. Due to symmetry of nodes and since $r_{ji}^{(2,2)} = 0$ if i , j are of different types, we re-write $C_{Ai}^{(2)^2}$ using (50) as,

$$C_{Ai}^{(2)^2} = U_{i,6} + U_{i,7}C_{Ai}^{(1)^2} \tag{63}$$

where

$$U_{i,6} = \begin{cases} 1 + \frac{n^{(p)}{\bar{r}_{\tilde{i}i}^{(2,2)}}^2 + {\bar{r}_{ii}^{(2,2)}}^2}{(E[c_i^{(2)}])^2}(U_{i,1} - 2(E[c_i^{(2)}])^2) \\ \qquad\qquad \text{, if } i \text{ is a primary node} \\ 1 + \frac{n^{(s)}{\bar{r}_{\tilde{i}i}^{(2,2)}}^2 + {\bar{r}_{ii}^{(2,2)}}^2}{(E[c_i^{(2)}])^2}(U_{i,1} - 2(E[c_i^{(2)}])^2) \\ \qquad\qquad \text{, if } i \text{ is a secondary node} \end{cases} \tag{64}$$

and

$$U_{i,7} = \begin{cases} \frac{n^{(p)}\bar{r}_{\tilde{i}i}^{(2,2)^2}+\bar{r}_{ii}^{(2,2)^2}}{(E[c_i^{(2)}])^2}U_{i,2}, & \text{if } i \text{ is a primary node} \\ \frac{n^{(s)}\bar{r}_{\tilde{i}i}^{(2,2)^2}+\bar{r}_{ii}^{(2,2)^2}}{(E[c_i^{(2)}])^2}U_{i,2}, & \text{if } i \text{ is a secondary node} \end{cases} \quad (65)$$

From Lemmas 1 and 2, we know routing probability and the average arrival-rate of class-2 jobs at each station. Due to symmetry of nodes (44), (57), (58) and (63) result in 8 linear equations in $C_{A,p}^{(2)^2}$, $C_{A,s}^{(2)^2}$, $C_{D,p}^{(2)^2}$, $C_{D,s}^{(2)^2}$, $C_{A,p}^{(1)^2}$, $C_{A,s}^{(1)^2}$, $E[f_p^{(2)^2}]$ and $E[f_s^{(2)^2}]$. Solving these system of linear equations, we obtain $C_{A,s}^{(1)^2}$. Then we find squared coefficient of variation of completion time of a class-2 job at secondary station k i.e $\frac{E[c_k^{(2)^2}]}{(E[c_k^{(2)}])^2} - 1$ using (49) and (50).

C. Average End-to-end Delay for Secondary Packets:

Now that we know the mean and coefficient of variation of the effective service time and inter-arrival time of a job at any secondary station k in the equivalent single-class G/G/1 -network, we can compute the average number of jobs at station, $\bar{Q}_k$ using (4). Since $\bar{Q}_k$ is equal to the average number of real secondary packets at node k and packet arrival-rate to k is $\lambda_k^{(2)}\bar{P}_{\text{dir}}^{(s)}$, the average system delay for secondary packets at k, using Little's theorem, is $\bar{D}_k = \frac{\bar{Q}_k}{\lambda_k^{(2)}\bar{P}_{\text{dir}}^{(s)}}$. The number of hops traversed by a secondary packet before being absorbed by another secondary node has a geometric distribution with parameter $q^{(s)}$. The average number of hops traversed is therefore $\frac{1}{q^{(s)}}$. Due to symmetry of secondary nodes the average end-to-end delay is the average system delay at k multiplied by the average number of hops i.e.,

$$D(n^{(s)}, n^{(p)}) = \bar{D}_k \frac{1}{q^{(s)}}. \quad (66)$$

REFERENCES

[1] "Office of the press secretary the white house. presidential memorandum: Unleashing the wireless broadband revolution." *http://www.whitehouse.gov/the-press-office/ presidential-memorandum-unleashing-wireless-broadband-revolution*.

[2] "Ears workshop report," *http://www.nsf.gov/mps/ast/ears _workshop_final_report_ce_final_corr.pdf*.

[3] D. Das and A. Abouzeid, "Delay analysis of multihop cognitive radio networks using network of virtual priority queues," in *(presented at) Wireless Commun. and Networking Conference (WCNC)*, April 2014.

[4] J. Andrews, "Seven ways that hetnets are a cellular paradigm shift," in *IEEE Commun. Magazine*, vol. 51, no. 3, March 2013, pp. 136–144.

[5] B. Lorenzo and S. Glisic, "Context-aware nanoscale modeling of multicast multihop cellular networks," in *IEEE/ACM Trans. on Networking*, vol. 21, no. 2, April 2013, pp. 359–372.

[6] P. Blasco, M. Bennis, and M. Dohler, "Backhaul-aware self-organizing operator-shared small cell networks," in *IEEE Int. Conference Communications (ICC)*, June 2013, pp. 2801–2806.

[7] T. Czachrski, T. Nycz, and F. Pekergin, "Diffusion approximation models for transient states and their application to priority queues," in *International Journal On Advances in Networks and Services*, vol. 2, no. 2, Dec 2009, pp. 205–217.

[8] G. Bolch, S. Greiner, H. d. Meer, and K. S. Trivedi, *Queueing Networks and Markov Chains*. Wiley-Interscience, 2005.

[9] S. Wang, J. Zhang, and L. Tong, "Delay analysis for cognitive radio networks with random access: A fluid queue view," in *Proc. IEEE INFOCOM*, 2010, pp. 1–9.

[10] R.-R. Chen and X. Liu, "Delay performance of threshold policies for dynamic spectrum access," in *IEEE Trans. Wireless Commun.*, vol. 10, no. 7, 2011, pp. 2283–2293.

[11] F. Mehmeti and T. Spyropoulos, "Who interrupted me? analyzing the effect of pu activity on cognitive user performance," in *Proc. ICC*, June 2013, pp. 2874–2879.

[12] A. Azarfar, J.-F. Frigon, and B. Sansò, "Priority queueing models for cognitive radio networks with traffic differentiation," *arXiv preprint arXiv:1203.6413*, 2012.

[13] I. Suliman and J. Lehtomaki, "Queueing analysis of opportunistic access in cognitive radios," in *Proc. IEEE Int. Workshop Cognitive Radio and Advanced Spectrum Management (CogART)*, 2009, pp. 153–157.

[14] H. Tran, T. Q. Duong, and H.-J. Zepernick, "Average waiting time of packets with different priorities in cognitive radio networks," in *Proc. IEEE Int. Symp. Wireless Pervasive Computing (ISWPC)*, May 2010, pp. 122 –127.

[15] C. Zhang, X. Wang, and J. Li, "Cooperative cognitive radio with priority queueing analysis," in *Proc. IEEE Int. Conference Commun. (ICC)*, June 2009, pp. 1–5.

[16] C. Do, N. Tran, and C. seon Hong, "Throughput maximization for the secondary user over multi-channel cognitive radio networks," in *Int. Conference Information Networking (ICOIN)*, Feb. 2012, pp. 65–69.

[17] W. Ren, Q. Zhao, and A. Swami, "On the connectivity and multihop delay of ad hoc cognitive radio networks," in *Proc. IEEE ICC*, 2010, pp. 1 –6.

[18] O. Simeone, Y. Bar-Ness, and U. Spagnolini, "Stable throughput of cognitive radios with and without relaying capability," in *IEEE Trans. Commun.*, vol. 55, no. 12, 2007, pp. 2351–2360.

[19] A. Fanous and A. Ephremides, "Stable throughput in a cognitive wireless network," in *IEEE J. Sel. Areas Commun.*, vol. 31, no. 3, 2013, pp. 523–533.
[20] I. Krikidis, J. Laneman, J. Thompson, and S. Mclaughlin, "Protocol design and throughput analysis for multi-user cognitive cooperative systems," in *IEEE Trans. on Wireless Commun.*, vol. 8, no. 9, September 2009, pp. 4740–4751.
[21] I. Krikidis, N. Devroye, and J. Thompson, "Stability analysis for cognitive radio with multi-access primary transmission," in *IEEE Trans. Wireless Commun.*, vol. 9, no. 1, 2010, pp. 72–77.
[22] A. El-Sherif, A. Sadek, and K. Liu, "Opportunistic multiple access for cognitive radio networks," in *IEEE J. Sel. Areas Commun.*, vol. 29, no. 4, 2011, pp. 704–715.
[23] A. E. Shafie and T. Khattab, "Energy-efficient cooperative relaying protocol for full-duplex cognitive radio users and delay-aware primary users," in *International Conference on Computing, Netw. and Commun. (ICNC)*, Feb 2015, pp. 207–213.
[24] A. El Shafie, A. Sultan, and T. Khattab, "Maximum throughput of a secondary user cooperating with an energy-aware primary user," in *12th Int. Symposium on Modeling and Optimization in Mobile, Ad Hoc, and Wireless Networks (WiOpt)*, May 2014, pp. 287–294.
[25] R. Urgaonkar and M. Neely, "Opportunistic cooperation in cognitive femtocell networks," *IEEE Journal on Selected Areas in Communications*, vol. 30, no. 3, pp. 607–616, 2012.
[26] E. Matskani, N. Chatzidiamantis, L. Georgiadis, I. Koutsopoulos, and L. Tassiulas, "Optimal primary-secondary user cooperation policies in cognitive radio networks," *arXiv preprint arXiv:1307.5613*, 2013.
[27] N. Bisnik and A. A. Abouzeid, "Queuing network models for delay analysis of multihop wireless ad hoc networks," in *Ad Hoc Netw.*, vol. 7, no. 1. Elsevier, Jan 2009, pp. 79–97.
[28] D. Das and A. A. Abouzeid, "Spatial-temporal queuing theoretic modeling of opportunistic multi-hop wireless networks with and without cooperation." [Online]. Available: http://www.ecse.rpi.edu/homepages/abouzeid/preprints/rev1.pdf
[29] P. Gupta and P. R. Kumar, "The capacity of wireless networks," in *IEEE Trans. Inf. Theory*, vol. 46, no. 2, 2000, pp. 388–404.
[30] A. Kumar, D. Manjunath, and J. Kuri, "Communication networking: an analytical approach." Elsevier, 2004.
[31] T. Spyropoulos, K. Psounis, and C. S. Raghavendra, "Spray and wait: an efficient routing scheme for intermittently connected mobile networks," in *Proc. ACM Special Interest Group on Data Commun. Workshop DTNs*, 2005, pp. 252–259.
[32] D. Braginsky and D. Estrin, "Rumor routing algorithm for sensor networks," in *Proc. First ACM Int. Workshop on Wireless sensor networks and applications*, 2002, pp. 22–31.
[33] B. Karp and H.-T. Kung, "Gpsr: Greedy perimeter stateless routing for wireless networks," in *Proc. 6th Annual International Conference on Mobile Computing and Networking, MobiCom 00*. ACM, 2000, pp. 243–254.
[34] E. W. Weisstein, "Circle-circle intersection," *From MathWorld–A Wolfram Web Resource. http://mathworld. wolfram. com/Circle-CircleIntersection. html*, 2009.

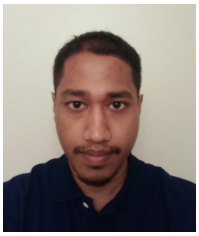

Dibakar Das received the B.Tech degree in Electrical Engineering from Indian Institute of Technology Madras (IITM), India, in 2008 and and MS degree in Computer Engineering from Texas AM University, College Station, in 2011, respectively. He is currently working toward a Ph.D. degree in Electrical, Computer and Systems Engineering Department, Rensselaer Polytechnic Institute, Troy, NY. His research interests include wireless networks, cooperative communications and cognitive radios.

Alhussein A. Abouzeid received the BS degree with honors from Cairo University, Egypt, in 1993, and the MS and PhD degrees from the University of Washington, Seattle, in 1999 and 2001, respectively, all in electrical engineering. From 1993 to 1994, he was with the Information Technology Institute, Information and Decision Support Center, The Cabinet of Egypt, where he received a degree in information technology. From 1994 to 1997, he was a project manager at Alcatel Telecom. He held visiting appointments with the aerospace division of AlliedSignal (currently Honeywell), Redmond, Washington, and Hughes Research Laboratories, Malibu, California, in 1999 and 2000, respectively. He is currently an associate professor with the Electrical, Computer and Systems Engineering Department, Rensselaer Polytechnic Institute, Troy, NY. He is also a visiting Professor and Finnish Distinguished Professor (FiDiPro) Fellow with University of Oulu, Finland. He served as a program director with US National Science Foundation from 2008 till 2010, where he was responsible for the Networking Technologies and Systems program, and he co-founded the Enhancing Access to Radio Spectrum (EARS) program. He is co-directing WiFiUS: Virtual Institute for Wireless Research between US and Finland, which is an NSF SAVI project for research collaboration between 20 US and Finnish institutions. He is a Senior Member of IEEE and serves/served on various conferences organization committees and editorial boards of several journals including IEEE Transaction on Wireless Communications and IEEE Wireless Communications Magazine. He is a recipient of the Faculty Early Career Development Award (CAREER) from the NSF in 2006.